Eur. Phys. J. AP **14**, 107–114 (2001)

THE EUROPEAN PHYSICAL JOURNAL APPLIED PHYSICS

In situ characterisation of non linear capacitors

L. Laudebat[1], V. Bley[1], T. Lebey[1,a], H. Schneider[2], and P. Tounsi[3]

[1] Laboratoire de Génie Électrique de Toulouse - Université Paul Sabatier, 118 route de Narbonne, 31062 Toulouse Cedex 4, France
[2] Laboratoire d'Électrotechnique et d'Électronique Industrielle INP-ENSEIIHT, 2 rue Camichel, 31062 Toulouse Cedex, France
[3] Laboratoire d'Analyse et d'Architecture des Systèmes du CNRS, 7 avenue du Colonel Roche, 31077 Toulouse Cedex 4, France

Received: 27 October 2000 / Revised and Accepted: 19 March 2001

Abstract. Multilayers ceramic capacitors (MLCC) presenting non linear behaviours of their $C(V)$ characteristics may have interesting applications in power electronics. Most of them have already been described. Nevertheless, the choice of a particular type instead of another one is all the more so difficult since, on one hand the physical mechanisms able to explain this behaviour is far from being understood. On the other hand, $C(V)$ characteristics are in general obtained for low voltage values different from the ones they are going to be involved in. In this paper, direct *in situ* characterisations of different $BaTiO_3$ based capacitors commercially available are achieved. The role of the capacitors' type (X7R,Z5U), of the temperature and of the voltage waveform (and more particularly its polarity) is demonstrated. Temperature values up to 200 °C are measured during normal operations in a RCD dissipative snubber without any alterations of the $C(V)$ characteristics. All these results are discussed as regards the main physical properties of the constitutive materials in order to reach an optimisation of their use through an appropriate dimensioning.

PACS. 77.22.-d Dielectric properties of solids and liquids – 77.80.-e Ferroelectricity and antiferroelectricity – 77.84.-s Dielectric, piezoelectric, ferroelectric, and antiferroelectric materials

1 Introduction

Multilayer ceramic capacitors (MLCC) are used for long time in low and medium power applications. This is mainly due to their high value of permittivity rather than to their breakdown field. For example, barium titanate based multilayer capacitors, classified as type II components, present a reduced size, leading to a high value of capacitance per unit of volume. They also present an excellent ability to withstand stresses for a long period of time. Nevertheless, changes in the dielectric constant, with either temperature or applied voltage, have very often limited their use.

However, they are the objects of a considerable amount of interest over the last few years in power electronics (PE) applications. As a matter of fact, some circuits of power electronics need these non-linear behaviours *versus* the applied voltage (resonant inverters, snubbers, ...) [1–3]. It has recently been demonstrated that integrated in resistance capacitance diode (RCD) dissipative snubber switching circuits, they allow, to limit the overvoltages during switching, to increase the switching frequency and to improve the electromagnetic compatibility [4]. Another application consists in introducing them in series resonance inverters allowing a simple adjustment of the power by change of their bias polarisation [5]. Nevertheless, their use is limited due to the limited understanding of the physical mechanisms driving their non linear behaviours. Even if lot has already been written on such ferroelectric materials [6–10] few is known on the possibility to transfer these physical characterisations, mainly developed on material samples, to applications involving components.

For example, most of the electrical characterisations presented in the literature are obtained for low level ac signal superimposed to a high DC voltage. Such a characterisation is far from being representative of PE stresses. The aim of this paper is to achieve *in situ* characterisations (*i.e.* in a system of PE) to compare them to the ones obtained in the classical approach and derived from these measurements. The comparison of different commercially available components is also achieved as regards their characteristics. At last a dimensioning optimisation of a snubber using such capacitors is proposed.

2 Experimental set up and definitions

A. Experimental

In situ characterisations of the capacitors under study are performed using a buck. It behaves as a middle point voltage source (magnitude up to 1000 V) and as a current source (during switching, thanks to a dipole L, R) (see Fig. 1).

[a] e-mail: lebey@lget.ups-tlse.fr

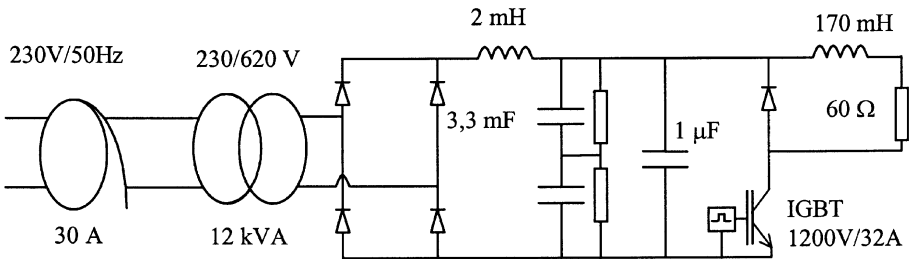

Fig. 1. Schematic representation of the buck used to perform characterisation.

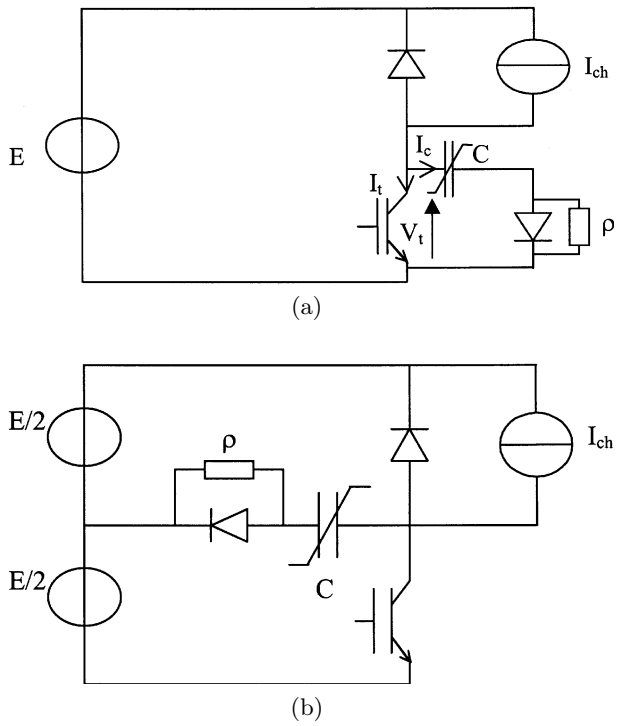

Fig. 2. The two type of circuits used to study the impact of (a) unipolar and (b) bipolar voltage waveform.

Since our goal is to characterise ceramic capacitors under voltage met in PE applications, two different electrical configurations are studied. The first one is a classical RCD dissipative snubber switching circuit, whereas the second one is used to study the impact of polarity reversal (as it is the case in serial resonant inverters). These two type of circuits are summarised in Figure 2 whereas Figure 3 presents current waveforms during turn-off switching for the two previous configurations.

At last different types of MLCC corresponding to the EIA (Electronic Industries Association) standard (Z5U, X7R, Y5V, 2F4) from different manufacturers are used. In this paper, the results are focused on X7R et Z5U components provided by two different manufacturers (A and B). In a first step, spectrofluorometry X measurements are performed and their results, summarised in Table 1, describe the different elements used for their realisation.

B. Definitions

For such non linear capacitors, the classical relationship between current and voltage does not stand anymore and must be rewritten as:

$$I = \frac{\partial V}{\partial t}\left(C + V\frac{\partial C}{\partial V}\right) = C^*\frac{\partial V}{\partial t}$$

where C is the "magnitude capacitance" defined as $Q = CV$ and C^* the "dynamic capacitance" defined as the local $\mathrm{d}Q/\mathrm{d}V$. These definitions are clearly explained in Figure 4 [11].

During our experiments, the following quantities ($\mathrm{d}V/\mathrm{d}t$, $i(t)/(\mathrm{d}V/\mathrm{d}t)$, $Q(t)$, $Q(t)/V$) are measured. They allow us to derive the values of C^* and C *vs.* the applied voltage and the time of voltage application for the different components under study (Fig. 5).

3 Results and discussions

A. Experimental results

Figure 6 to Figure 8 present the main trends derived from the measurements performed in the buck for the different components under study under unipolar voltage after drift has been stabilised (15 min).

First of all, the maximum of non linearity ($\mathrm{d}C/\mathrm{d}V$) appears to be dependent on the material nature. The voltage corresponding to this maximum of non linearity will be a dimensioning parameter of the snubber. For example, the voltage range may be limited to 0–50 V for Y5V components (since its maximum of non linearity (MNL) is in between 10 to 20 V) whereas X7R samples seem to be able to target higher voltage applications (MNL between 30 to 60 V).

In a second step, it has to be noted that the C^* behaviours are the same than the ones measured under low level ac signal superimposed to a high DC voltage. Such a result may appear interesting for at least two reasons:

– to size the converter before it is built *via* an off line characterisation under small signal. Hence the choice of the appropriate characteristic could be achieved prior to the converter building. Each application would have therefore, its own $C(V)$ characteristic as regards the applied stresses.

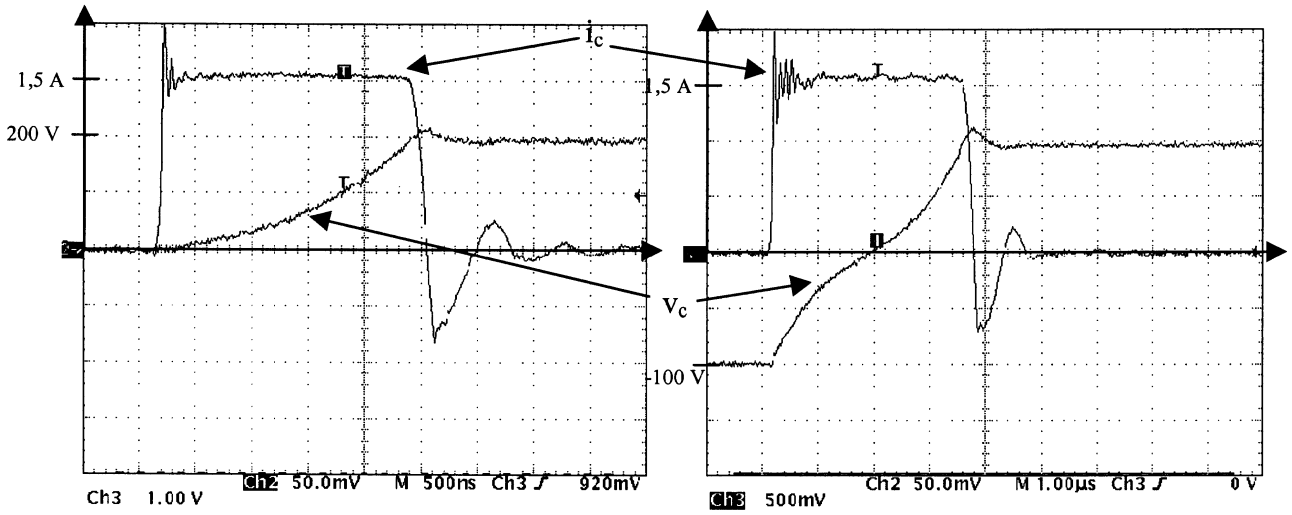

Fig. 3. Typical current and voltage waveforms applied to X7R 47 nF components (a) unipolar and (b) bipolar voltage waveform.

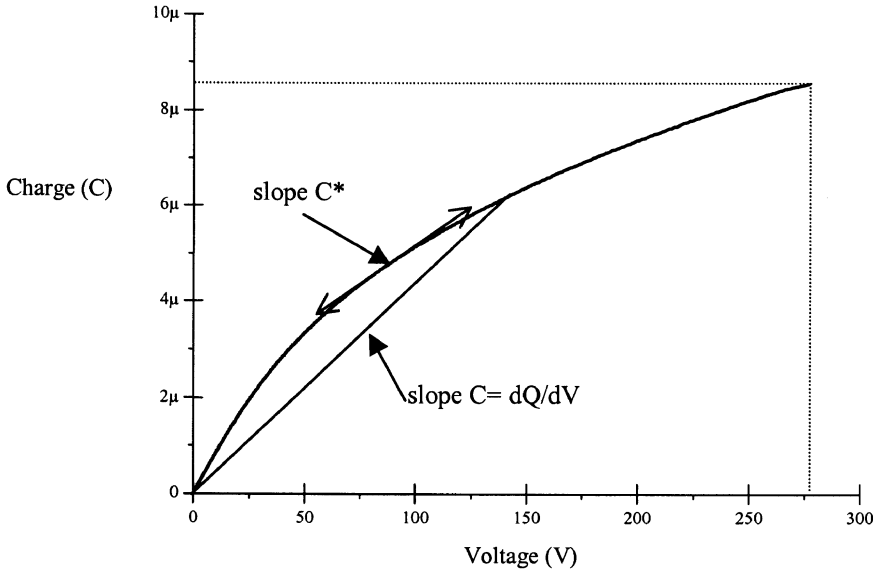

Fig. 4. Definition of C and C^*.

Table 1. Summary of the different elements present in the components under study using spectrofluorometry X measurements.

	X7R A	X7RB	Z5U A	Z5U B
Dielectric	Ba, Ti, Nb	Ba, Ti, Nb	Ba, Ti, Zr	Ba, Ti, Zr, Pb
Electrodes	Ag, Pd	Ag, Pd	Ag, Pd	Ni
Ending	Ag, Pd, Zn	Ag, Pd	Ag, Pd, Zn, Bi	Cu
Connections	Cu	Fe Ni	Cu	Fe Ni
Encapsulation	Cerfeuil	Br, Cu	Cerfeuil	BrCu

– to develop an appropriate maintenance of the system through on line measurements. As a matter of fact, if we suppose that the behavior of the component under stress has been established under small signal characterization, then it allows a better understanding of the physical mechanisms involved during aging. A transfer of this knowledge to the real system *via* the characteristic changes may be considered as a good indicator of the component' aging. Works must however be undertaken to confirm these assumptions.

However such an observation is true for a static description because, if the voltage is not removed, and whatever the components under study, drifts of these characteristics are observed. The largest drifts are observed under bipolar applied voltage (Fig. 9). At last, for some components (mainly Z5U manufacturer B) and whatever

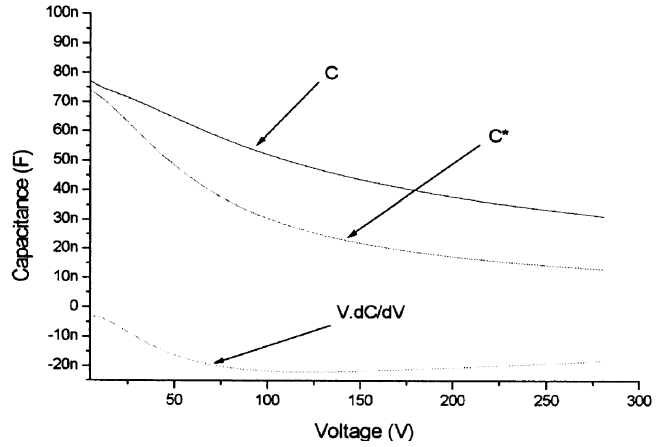

Fig. 5. Characteristics measured for each capacitor.

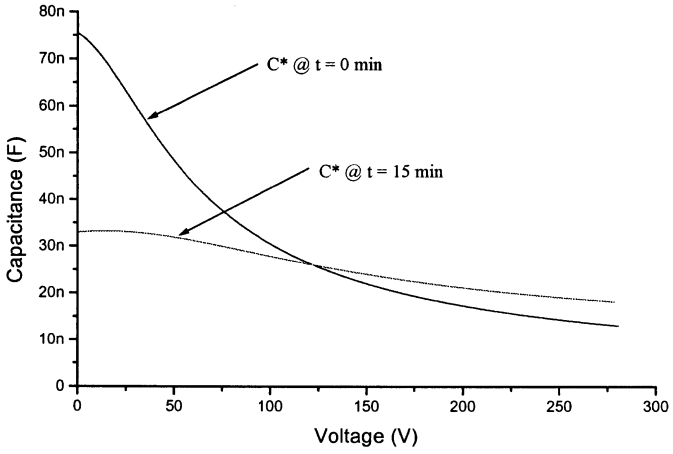

Fig. 6. Dynamic capacitance measured *vs.* time for Z5U components.

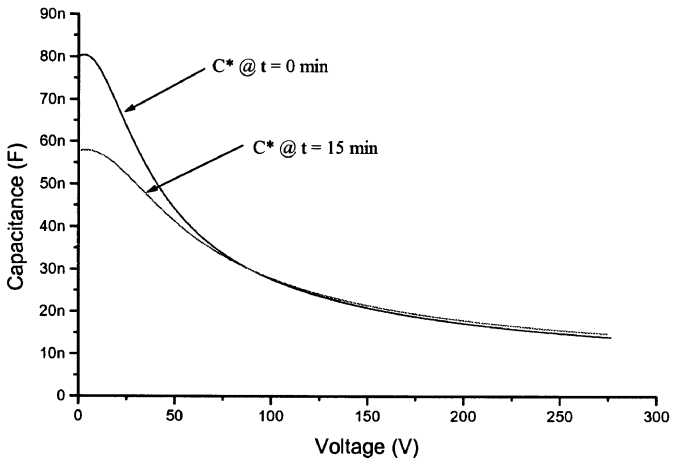

Fig. 7. Dynamic capacitance measured *vs.* time for X7R components.

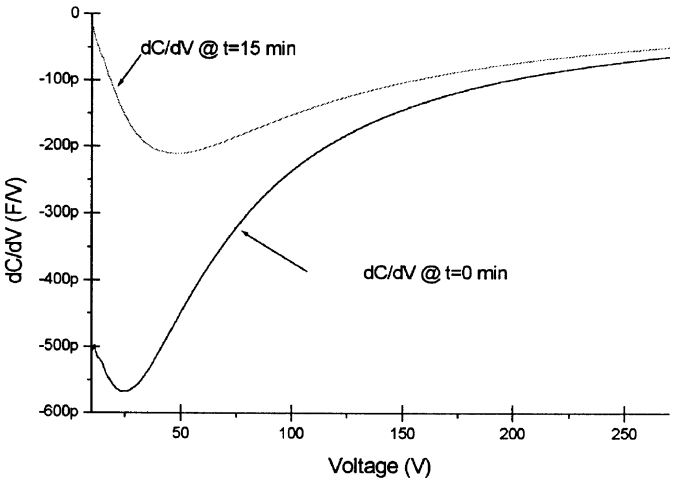

Fig. 8. Drift of maximum non linearity for X7R components.

the polarity of the applied voltage, these drifts lead to the failure of the capacitors and/or of the IGBT used. These faults appear briefly after voltage application: around 10 min under unipolar voltage and 1 min under the bipolar ones of the same characteristics (Magnitude $E = 500$ V, $(0 - E$ or $(E/2, -E/2)$, frequency ($f = 10$ kHz) and duty cycle R).

Taking into account these drifts for the components' choice, our study show that the X7R ones from manufacturer A appear to be the more relevant for these type of applications rather than any other material considered in this study.

All these results seems to depend on the material nature and more particularly on their thermal stability (according to EIA). The impact of the frequency increase has therefore to be studied. For different switching frequencies ($f = 500$ Hz, 1, 10, 15 kHz), a decrease in either the magnitude and dynamic capacitance is observed whatever the type of components considered. Note that the same trend is observed for a fixed frequency during an increase of the load current. These results seem to confirm the non negligible impact of the temperature on the dynamic behaviour of these components. Since it is often claimed that this last one is associated to their ferroelectric nature, the observed drifts could be associated to a temperature increase up to T_c (the Curie temperature). Then, for higher temperature values where the ferroelectricity has vanished, the non linear properties of these components would disappear. In order to confirm the last assumption, an IR camera, allowing surface thermal measurements, focused on the capacitor is used. This last one is placed vertically and perpendicular to the substrate where the other components are testing (see Fig. 10). Therefore, there is little or no interaction between the other components thermal increase during switching and the capacitor. X7R samples (capacity 100 nF) are studied for the different following conditions: two frequencies (10 and 20 kHz) for both unipolar and bipolar stresses. The current magnitude is 2 A.

Figure 11 gives an example of results obtained whereas Table 2 and Table 3 summarise the mean temperature values measured after drift stabilisation. $BaTiO_3$ thermal conductivity and the thickness between electrodes (10–20 μm) guarantee an homogeneous temperature after some minutes. Note that these values are not extreme values but statistical ones measured on different samples.

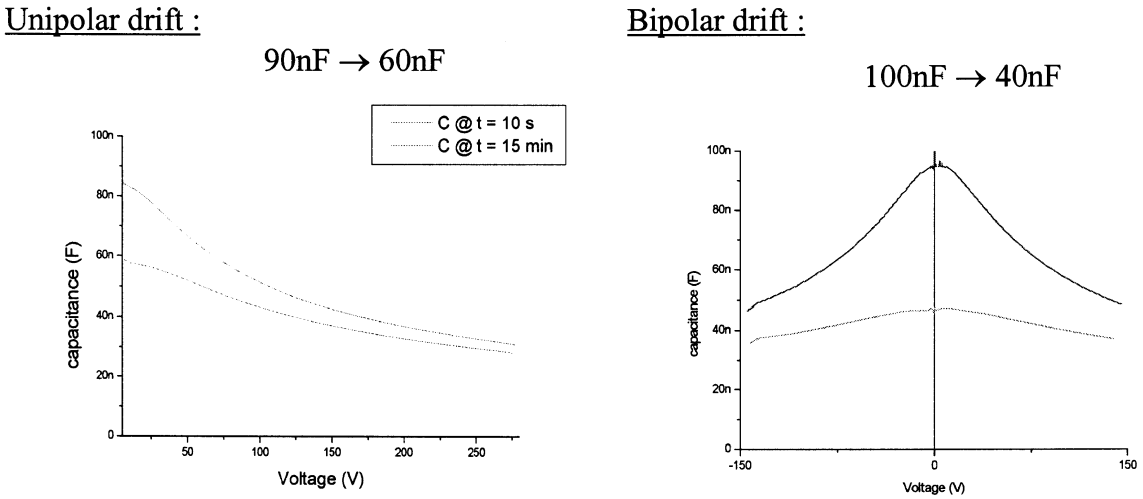

Fig. 9. Comparison between unipolar and bipolar mode.

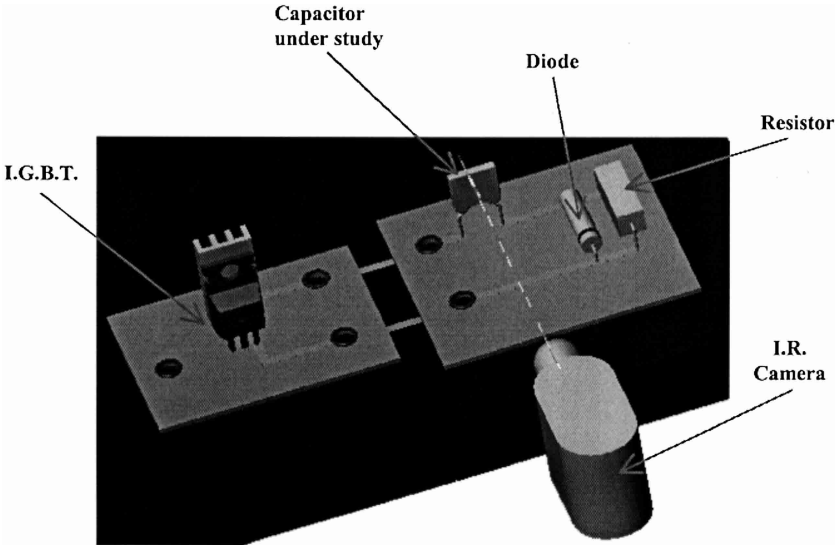

Fig. 10. Description of the physical layout for temperature measurements.

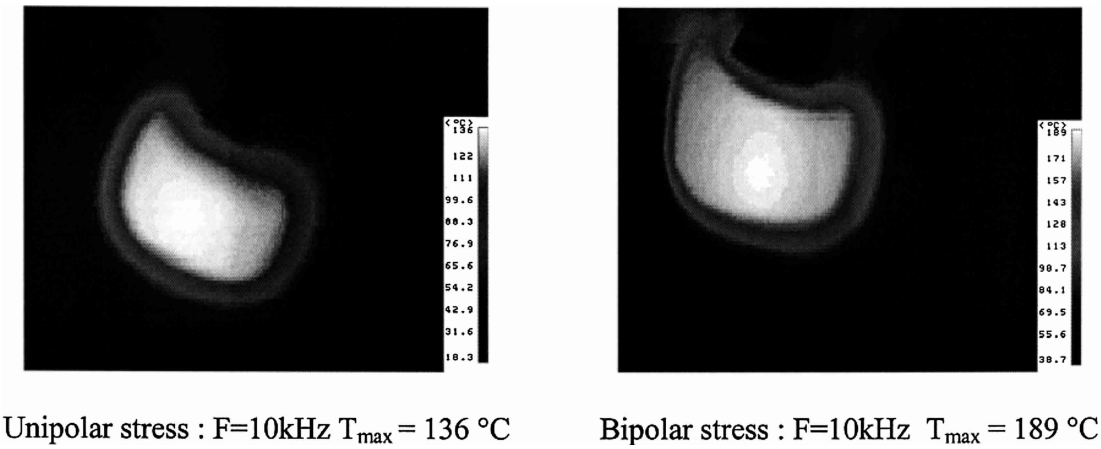

Fig. 11. Example of thermal acquisitions using IR camera for two voltage conditions.

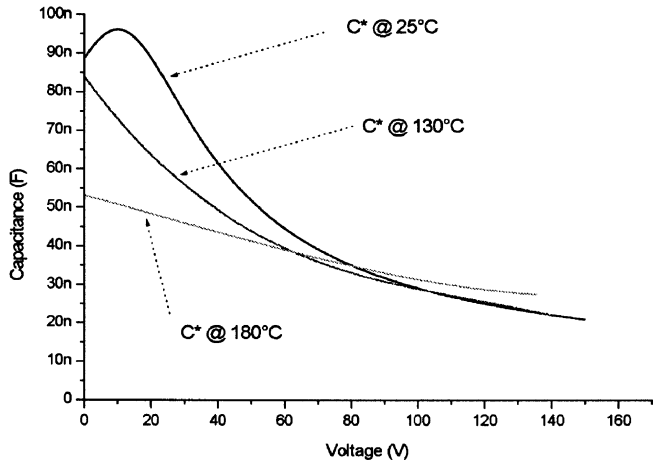

Fig. 12. Changes in the different measured characteristics of Z5U components during indirect heating for different temperatures.

Table 2. Mean values of the measured temperature during unipolar voltage application for X7R components.

Type	Frequency (kHz)	$T(^\circ\mathrm{C})$
X7R	10	140
X7R	20	200

Table 3. Mean values of the measured temperature during bipolar voltage application for X7R components.

Type	Frequency (kHz)	$T(^\circ\mathrm{C})$
X7R	10	190
X7R	20	270

Moreover the capacitor temperature is higher than the one measured on the other components (IGBT or resistor).

Such temperature values are very surprising. They are well above T_c and the material still present a non-linear behaviour! The correlation between ferroelectricity and non linear properties is therefore far from being demonstrated. Another confirmation of this non univocal relationship is given through an indirect heating of the components. The components are placed in an oven, and short cables lengths (in order to minimise inductance) link them to the buck outside. The different electrical measurements are performed after 30 min at the temperature under study.

For this study, the switching frequency and the current values are chosen in order that they do not lead to a temperature rise ($I = 0.5$ A and $f = 500$ Hz). An example of result is given in Figure 12 leading to the conclusions that these components still present non linear properties for temperature well above the Curie temperature. Their use under extreme conditions seems therefore possible.

In the following, we propose and discuss reasons able to explain both the increase in temperature and the non linear properties observed during working.

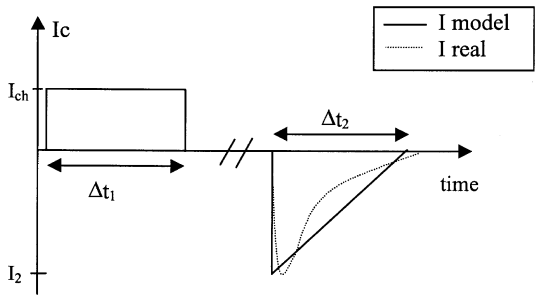

Fig. 13. Typical current waveforms applied to capacitor during a period.

B. Temperature vs. capacitors

Origins of the temperature increase may be either extrinsic and/or intrinsic to the materials. Intrinsic means that it is associated to the material nature. For ferroelectric materials, two aspects have to be considered: dielectric losses and hysteresis losses. Nevertheless, for the frequency and temperature under studies, neither dielectric losses (no dielectric relaxation is observed in this frequency range) nor hysteresis losses (the surface of the hysteresis loop is decreasing with frequency) are able to lead to the observed overheating of the components.

Extrinsic phenomena are associated to the environment of the component. Therefore, it is possible to assume that the overheating is due to the type of electrodes which, despite the low thermal conductivity of the dielectric (around 2.5 W/m K), could allow the material to reach the electrode temperatures. This last one is a function of the square of the current and of the resistivity of the electrode's material. Such an approach is able to explain the difference between Z5U samples A and B (see Tab. 1) due to the type of the metal used and therefore to the difference in their resistivities. The resistivity of Ni ($\sim 6.9 \times 10^{-6}\ \Omega\,\mathrm{cm}$) is higher than the resistivity of AgPd ($\sim 1 \times 10^{-6}\ \Omega\,\mathrm{cm}$). The current is determined using an approximation presented in Figure 13. It is considered constant and equal to I_{ch} during Δt_1 and then varies during Δt_2 from I_2 to 0 leading to:

$$I_{rms} = \sqrt{f\left(\int_0^{\Delta t_1} I_{ch}^2 \mathrm{d}t + \int_0^{\Delta t_2} I_2 - \frac{I_2}{\Delta t_2}\mathrm{d}t\right)}.$$

For a voltage magnitude of 250 V, a load current of 2 A, a frequency of 10 kHz, the results are $I = 1.2$ A and 0.75 A for X7R components A and B respectively, and 0.5 A and 0.7 A for Z5U components A and B. At last, it has to be noted that the current is strongly dependent on the switching frequency and on the load current value.

However, even if the dependence of the metal resistivity with the temperature is taken into account, this approach is not sufficient to explain the temperature differences ($\sim 50\ ^\circ$C) induced by the application of unipolar and bipolar voltage waveforms since the current difference is for the previous buck characteristics near 0.07 A.

Other reasons mainly associated to the material itself have to be derived.

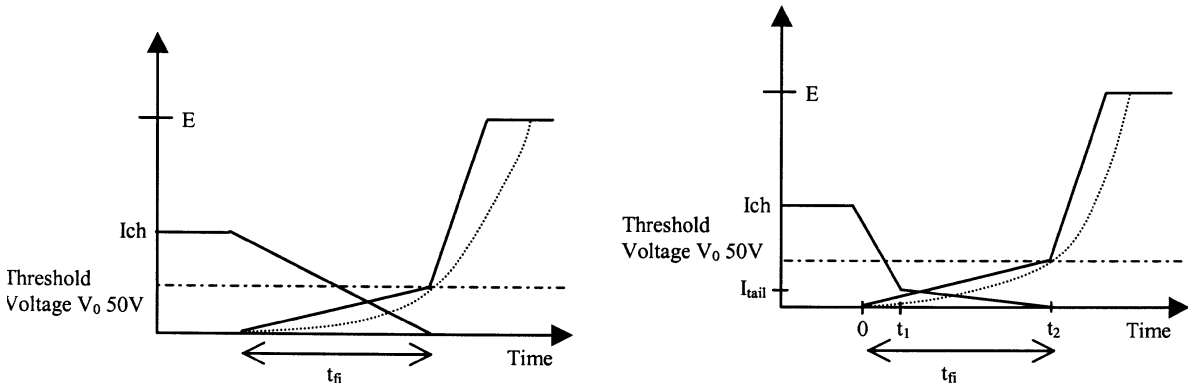

Fig. 14. Example of an ideal switching turn off (MOS -a and IGBT -b) allowing the definition of the different parameters.

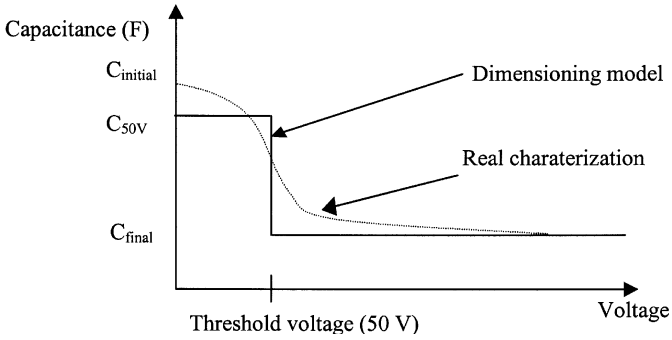

Fig. 15. $C(V)$ ideal profile.

C. Non linear properties

As mentioned previously, it is often claimed that the non linear properties of barium titanate based ceramic capacitors are associated to their ferroelectricity. Our results seem to indicate the contrary: the working temperature is far above T_c and the capacitances are still presenting non linear behaviours. Other reasons, involving intrinsic dielectric properties have to be considered. Among them, space charge injection and built up has to be taken into account. Such an assumption has already been implicitly made by van Wyk [7]. Different observation are in favour of it. On one hand, in most of cases the drift observed is not reversal. The cooling of the samples is unable to restore their initial properties. The only way to make disappear the effects of voltage application is to apply bipolar voltages at very high temperatures. On the other hand, the non linearity depends on the nature of the electrodes (electronic affinity) and does not seem to depend on the material state (ferroelectric or paraelectric).

Works must now be undertaken to confirm space charge existence. Since, if it is responsible of the non linearity observed, this phenomenon which may be controlled, could give the opportunity to obtain an appropriate $C(V)$ profile as regards the envisaged applications.

D. Dimensioning a snubber using non linear capacitance

Taking into account the different previous results a question arises: how to dimension a RCD snubber dissipative circuit using such components?

An example of an ideal switching is given in Figure 14 allowing the definition of the different parameters necessary for the following demonstration. A model of the capacity associated to this type of switching is given in Figure 15 [1–3]. C_{init}, C_{final}, $C_{50\text{V}}$ correspond respectively to the initial value, the final value (previously named C^*) of the capacity and to the maximum of $\mathrm{d}C/\mathrm{d}V$ (Fig. 8). All values are defined after drift stabilisation. When dimensioning such a snubber, the goal is to force the voltage characteristics to pass through the point (t_{fi}, V_0) of Figure 14a (for MOS transistor turn off switching) corresponding to a change in $\mathrm{d}V/\mathrm{d}t$ slope taking also into account the changes in the $C(V)$. This leads to:

$$i_t = I_{\text{ch}} - \frac{I_{\text{ch}}}{t_{\text{fi}}} \times t. \tag{1}$$

Hence current and the voltage on the capacitor plates are:

$$i_{\text{c}} = \frac{I_{\text{ch}}}{t_{\text{fi}}} \times t \tag{2}$$

$$V_{\text{c}} = \frac{1}{C_{50\text{V}}} \int_0^{t_{\text{fi}}} \frac{I_{\text{ch}}}{t_{\text{fi}}} \times t\mathrm{d}t \tag{3}$$

$$C_{50\text{V}} = \frac{I_{\text{ch}} \times t_{\text{fi}}}{2V_0} \quad \text{for a MOS.} \tag{4}$$

In the particular case of an IGBT commutation (see Fig. 14b):

for 0 to t_1:

$$i_t = I_{\text{ch}} - \frac{I_{\text{ch}} - I_{\text{tail}}}{t_1} \times t \tag{5}$$

between t_1 and t_2:

$$i_t = I_{\text{tail}} - \frac{I_{\text{tail}}}{t_2 - t_1} \times t \tag{6}$$

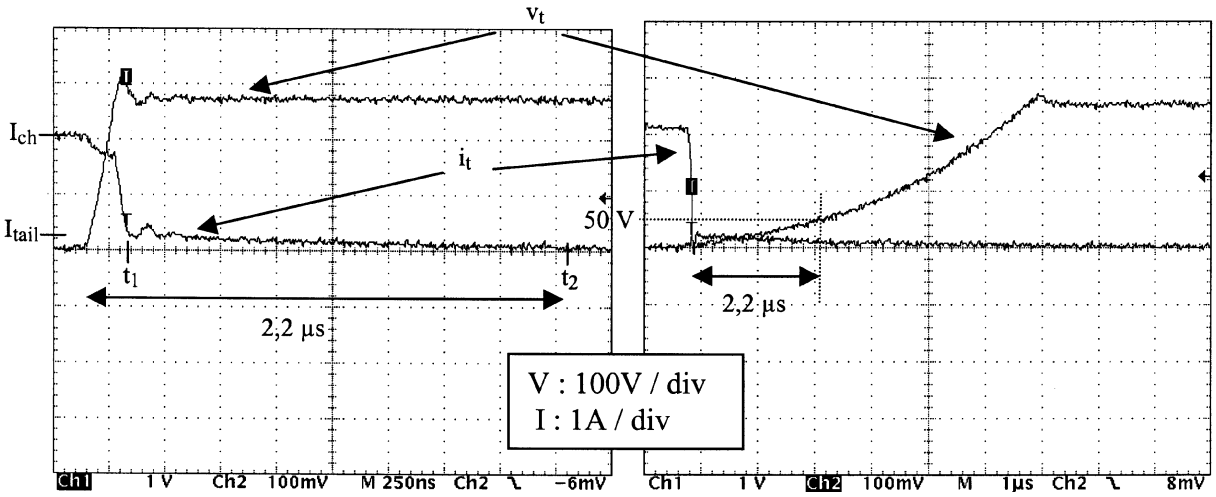

Fig. 16. Example of a correct snubber dimensioning.

therefore:

$$i_c = I_{ch} - i_t \tag{7}$$

$$V_c = \frac{1}{C_{50V}} \left(\int_0^{t_1} \frac{I_{ch} - I_{tail}}{t_1} dt + \int_{t_1}^{t_2} \left(I_{ch} - I_{tail} + \frac{I_{tail}}{t_2 - t_1} \right) dt \right) \tag{8}$$

$$C_{50V} = \frac{I_{ch} t_2}{V_0} - \frac{I_{tail} t_2}{2V_0} - \frac{I_{ch} t_1}{2V_0} + \frac{I_{tail} t_1}{V_0} \tag{9}$$

$$C_{50V} \cong \frac{I_{ch} \times t_{fi}}{V_0} \quad \text{for an IGBT or GTO.} \tag{10}$$

Equation (10) as a first order approximation of equation (9) allows a correct determination of C_{50V}. This approximation is all the more true since $I_{tail} \ll I_{ch}$ and $t_1 \ll t_{fi}$ (Fig. 16). This approach allows a quasi ideal use of the snubber as may be seem in Figure 16 for an IGBT.

4 Conclusions

The aim of this paper was to perform *in situ* measurements of the characteristics of non linear capacitances using a buck. We have clearly demonstrated that:

- The classical low level ac voltage superimposed to a high DC voltage characterisation generally performed is in most of cases sufficient to determine the C-V behaviour. By the same way a direct *in situ* characterisation may be sufficient for determining the component ability to be used in its application;
- Most of the components studied have a maximum non linearity for voltage magnitude below 100 V;
- Application of bipolar high frequency voltage waveforms may lead to the failure of the weakest components (Z5U B);
- The working temperature may reach a value up to 200 °C and the non-linear behaviour of the components is still existing;
- Using non linear capacitors in snubber circuits decreases switching times and stored energies (and therefore those dissipated in the resistor) by at least 50% as compared to linear ones. It has to be noticed however that despite their quality, ceramic capacitors present dielectric losses larger than the ones observed in polymer based capacitors. The impact of these losses on the dynamic performance are not so simple to appreciate. In a first approximation, it may be argued that from a circuit point of view, they may be considered as negligible.

Works are still in progress in order to determine the reasons of the non linear behaviour, which seems to be mainly related to space charge injection and built up, and to reach an appropriate dimensioning of such components on the basis of the knowledge of the origin of their non linear behaviour.

References

1. C.G. Steyn, J.D. Van Wyk, IEEE Trans. Ind. Appl. **IA-22**, 471 (1986).
2. C.G. Steyn, J.D. Van Wyk, IEEE Trans. Ind. Appl. **25**, 226 (1989).
3. G. Friegen, J.D. Van Wyk, IEEE Trans. Power Electron. **7**, 425 (1992).
4. N. Aouda, Les condensateurs en électronique de puissance, Ph.D. dissertation, Chap. 4, 1995, Toulouse - France.
5. K. Harada, A. Katsuki, M. Fujiwara, H. Nakajima, H. Matsushita, IEEE Trans. Power Electron. **8**, 404 (1993).
6. G.A. Smolenskii, Soviet Phys. Solid State **1**, 147 (1959).
7. C.K. Campbell, J.D. Van Wyk, M.F.K. Holm, IEEE Trans. Components Packaging and Manufacturing Technol. - Part A. **18**, 226 (1995).
8. N. Benhamla, *Electroceramics IV, 4th International Conference on Electronic Ceramics and Application, Germany, Sept 1994*, p. 101.
9. E.A. Little, Phys. Rev. **98**, 978 (1995).
10. W. Jackson, *The insulation of electrical equipment* (Chapman and Hall Ltd, London, 1954), p. 75.
11. G.R. Love, J. Am. Ceram. Soc. **73**, 323 (1990).